Electronic Supplementary Material (ESI) for Nanoscale.

Supporting Information

N-doped Porous Carbon Network with Multidirectional Structure as Highly Efficient Metal-Free Catalysts for Oxygen Reduction Reaction

Hyunsu Han[a,b], *Yuseong Noh*[a,b], *Yoongon Kim*[c], *Won Suk Jung*[a,b], *Seongmin Park*[a,b], and *Won Bae Kim*[a,b]*

[a] Department of Chemical Engineering, Pohang University of Science and Technology (POSTECH), 77 Cheongam-ro, Nam-gu, Pohang, Gyeongbuk, 37673, South Korea

[b] Institute for New and Renewable Energy, Pohang University of Science and Technology (POSTECH), 77 Cheongam-ro, Nam-gu, Pohang, Gyeongbuk, 37673, South Korea

[c] School of Materials Science & Engineering, Gwangju Institute of Science and Technology (GIST), 261 Cheomdan-gwagiro, Buk-gu, Gwangju 500-712, South Korea

* Corresponding author
Tel: 82-54-279-2397
Fax: 82-54-279-5528
E-Mail: kimwb@postech.ac.kr

Table S1. Textural properties of various N-doped porous carbons.

Sample	BET surface area ($m^2\ g^{-1}$)	Microporous area ($m^2\ g^{-1}$)	Total pore volume ($cm^3\ g^{-1}$)	Micropore volume[b] ($cm^3\ g^{-1}$)
NPC[a]	1026.6	605.6	1.046	0.648
NPC-800-0.5	833.4	516.7	0.769	0.498
NPC-800-1.5	637.2	407.8	0.664	0.418
NPC-700-1	1211.4	735.8	1.101	0.715
NPC-900-1	459.3	276.8	0.513	0.308

[a] Activation temperature = 800 °C; the weight ratio of KOH/PPyCS = 1

[b] Micropore volume is estimated by t-plot method.

Table S2. The chemical compositions of various N-doped porous carbons obtained by XPS.

Sample	C (%)	O (%)	N (%)	Graphitic N (%)	Pyridinic N (%)	Oxidized N (%)	Pyrrolic N (%)
NPC[a]	85.5	8.1	6.4	49.1	24.0	12.1	14.8
NPC-800-0.5	85.7	7.6	6.7	46.3	24.9	17.2	11.6
NPC-800-1.5	85.2	9.2	5.6	54.2	22.8	8.6	14.4
NPC-700-1	85.5	7.9	6.6	40.8	25.8	12.0	21.4
NPC-900-1	85.5	9.3	5.2	51.1	22.1	10.9	15.9

[a] Activation temperature = 800 °C; the weight ratio of KOH/PPyCS = 1

Table S3. Comparison of the ORR performances over the N-doped carbon-based catalysts in forms of metal-free N-doped carbons and metal-N-doped carbons in 0.1 M KOH electrolyte.

Sample	Onset potential (V vs RHE)	Half-wave potential (V vs RHE)	Limiting current density[a] (mA cm^{-2})	Electron transfer number	Stability[c] (test time, sec)	N doping content[b] (at. %)	BET surface area (m^2 g^{-1})	Synthesis method	Ref.
NPC	0.94	0.864	5.65	4.03	95.2 (50,000)	6.4	1026	KOH treatment /pyrolysis process	This work
NC900	0.83	-	4.0	3.3	-	2.70	2747	Pyrolysis process	S1
NPC-F	0.91	0.84	5.5	3.67-3.94	-	3.46	1375	Pyrolysis process	S2
Carbon nano shell	0.98	0.85	5.1	3.7	~93 (50,000)	3.71	1189	Nano-casting	S3
DCN-1000	0.94	0.85	4.21	3.72	88.7 (30,000)	8.3	~ 285	Pyrolysis process	S4
N-CNFs-800	0.93	-	5.7	3.7	93.2 (20,000)	6.94	230	Pyrolysis process	S5
NCG-1000	0.91[d]	0.737[d]	-	3.79	-	3.98	-	Pyrolysis process	S6
N-GNRs-A	0.91[d]	-	-	3.66-3.92	~ 78 (20,000)	2.81	617	Pyrolysis process	S7
NGA900	0.914	0.828	4.6	3.9	86 (35,000)	-	-	Pyrolysis process	S8
Fe-N/C-800	0.98	-	4.81	3.97	93.3 (10,000)	5.79	934.43	Hydro-thermal /pyrolysis process	S9
CoP-CMP800	0.857[d]	0.797[d]	4.62	3.85	-	7.5	~ 480	Template -free pyrolysis process	S10
Co_9S_8@ N-C	0.89	0.83	-	~ 4	85 (20,000)	3.45	110.8	Solvo-thermal process	S11

[a] Limiting current density is recorded at a rotation rate of 1600 rpm.

[b] N content is obtained from XPS spectra.

[c] Value of stability test indicates a relative current (%) obtained from chronoamperometry test.

[d] Conversion of reference electrode into RHE scale was based on the calibration results in this work and a reported paper [S12].

Reference for Table S3

[S1] A. Aijaz, N. Fujiwara and Q. Xu, *J. Am. Chem. Soc*., 2014, **136**, 6790.

[S2] Z. Xu, X. Zhuang, C. Yang, J. Cao, Z. Yao, Y. Tang, J. Jiang, D. Wu and X. Feng, *Adv. Mater*., 2016, **28**, 1981.

[S3] Y. Wang, A. Kong, X. Chen, Q. Lin and P. Feng, *ACS Catal*., 2015, **5**, 3887.

[S4] X. Li, J. Kang, Y. Dai, C. Dong, X. Guo and X. Jia, *Adv. Mater. Interfaces*, 2018, **5**, 1800303.

[S5] R. Li, X. Shao, S. Li, P. Cheng, Z. Hu and D. Yuan, *Nanotechnology*, 2016, **27**, 505402.

[S6] M. Wang, J. Wang, Y. Hou, D. Shi, D. Wexler, S. D. Poynton, R. C. T. Slade, W. Zhang, H. Liu and J. Chen, *ACS Appl. Mater. Interfaces*, 2015, **7**, 7066.

[S7] L. Chen, R. Du, J. Zhu, Y. Mao, C. Xue, N. Zhang, Y. Hou, J. Zhang and T. Yi, *Small,* 2015, **11**, 1423.

[S8] J. Li, Y. Zhang, X. Zhang, J. Han, Y. Wang, L. Gu, Z. Zhang, X. Wang, J. Jian, P. Xu and B. Song, *ACS Appl. Mater. Interfaces,* 2015, **7**, 19626.

[S9] Ding, L. Li, K. Xiong, Y. Wang, W. Li, Y. Nie, S. Chen, X. Qi and Z. Wei, *J. Am. Chem. Soc*., 2015, 137, **16**, 5414.

[S10] Z. S. Wu, L. Chen, J. Liu, K. Parvez, H. Liang, J. Shu, H. Sachdev, R. Graf, X. Feng and K. Müllen, *Adv. Mater*., 2014, **26**, 1450.

[S11] Z. Wu, J. Wang, M. Song, G. Zhao, Y. Zhu, G. Fu and X. Liu, *ACS Appl. Mater. Interfaces*, 2018, **10**, 25415.

[S12] V. Percec, C. H. Ahn, G. Ungar, D. J. P. Yeardley, M. Moller and S. S. Sheiko, *Nature*, 1998, **391**, 161.

Table S4. Comparison of the ORR performances over the N-doped carbon-based catalysts in forms of metal-free N-doped carbons and metal-N-doped carbons in acidic condition.

Sample	Onset potential (V vs RHE)	Half-wave potential (V vs RHE)	Limiting current density[a] (mA cm^{-2})	Electron transfer number	Stability[c] (test time, sec)	N doping content[b] (at. %)	BET surface area (m^2 g^{-1})	Synthesis method	Ref.
NPC	0.84	0.74	5.3	3.93	94.1 (50,000)	6.4	1026	KOH treatment /pyrolysis process	This work
NCS-800	0.72	0.4	3.3	3.90-3.98	~80 (~ 9,500)	9.1	646	Hydro-thermal /pyrolysis process	S1
CCa	0.76	0.37	-	-	-	9.2	1350	Pyrolysis process	S2
NPC-1000	0.818	0.698	5.85	3.82-3.99	< 90 (~20,000)	2.08	811	Pyrolysis process	S3
Co-Zn-ZIF/ GO-800[d]	0.85	-	4.2	~ 4	84 (10,800)	-	1170	Crystal growth/ pyrolysis process	S4
Fe-N/C-800[d]	0.77	0.6	4.88	3.95	-	5.79	934.43	Hydro-thermal/ pyrolysis process	S5
CPANI-Fe-NaCl[d]	-	~ 0.727	~ 5	~ 3.9	-	-	265.7	Salt crystalli zation process	S6
P-Fe-N-CNFs[d]	0.85	0.74	5.5	3.99	96 (10,000)	6.23	941	Multiplex templating process	S7
NPMEs[d]	0.824	0.748	4.43	3.84	-	2.26	267	Self-assembly /pyrolysis process	S8
Fe/SNC	-	0.77	~ 4.8	3.85	86 (3,000)	5.7	1032	Template casting process	S9
FePPy-900	0.814	0.74	5.7	3.5-4.0	87 (~ 4,200)	4.25	592.2	Pyrolysis/ leaching/st abilization process	S10
Fe-N-CC	0.8	0.52	-	3.8	-	5.88	1590	Vapor deposition polymeri zation/ pyrolysis process	S11

[a] Limiting current density is recorded at a rotation rate of 1600 rpm.
[b] N content is obtained from XPS analysis.
[c] Value of stability test indicates a relative current (%) obtained from chronoamperometry test.
[d] Electrolyte is 0.1 M $HClO_4$ aqueous solution.

Reference for Table S4

[S1] P. Chen, L. K. Wang, G. Wang, M. R. Gao, J. Ge, W. J. Yuan, Y. H. Shen, A. J. Xie and S. H. Yu, *Energy Environ. Sci.,* 2014, **7**, 4095.

[S2] G. A. Ferrero, A. B. Fuertes, M. Sevilla and M. M. Titirici, *Carbon*, *2016*, **106**, 179.

[S3] L. Ye, G. Chai and Z. Wen, *Adv. Funct. Mater*., 2017, **27**, 1606190.

[S4] J. Wei, Y. Hu, Y. Liang, B. Kong, J. Zhang, J. Song, Q. Bao, G. P. Simon, S. P. Jiang and H. Wang, *Adv. Funct. Mater*., 2015, **25**, 5768.

[S5] W. Niu, L. Liu, N. Wang, J. Liu, W. Zhou, Z. Tang and S. Chen, *J. Am. Chem. Soc*., 2015, **137**, 5555.

[S6] W. Ding, L. Li, K. Xiong, Y. Wang, W. Li, Y. Nie, S. Chen, X. Qi and Z. Wei, *J. Am. Chem. Soc.*, 2015, **137**, 5414.

[S7] B. C. Hu, Z. Y. Wu, S. Q. Chu, H. W. Zhu, H. W. Liang, J. Zhang and S. H. Yu, *Energy Environ. Sci.,* 2018, **11**, 2208.

[S8] J. Li, Y. Song, G. Zhang, H. Liu, Y. Wang, S. Sun and X. Guo, *Adv. Funct. Mater.,* 2017, **27**, 1604356.

[S9] H. Shen, G. E. Eduardo, J. Ma, K. Zang, J. Luo, L. Wang, S. Gao, X. Mamat, G. Hu, T. Wagberg and S. Guo*, Angew.Chem. Int. Ed.,* 2017, **56**, 13800.

[S10] T. N. Tran, M. Y. Song, K. P. Singh, D. S. Yang and J. S. Yu, *J. Mater. Chem. A*, 2016, **4**, 8645.

[S11] G. A. Ferrero, K. Preuss, A. Marinovic, A. B. Jorge, N. Mansor, D. J. L. Brett, A. B. Fuertes, M. Sevilla and M. M. Titirici, *ACS Nano*, 2016, **10**, 5922.

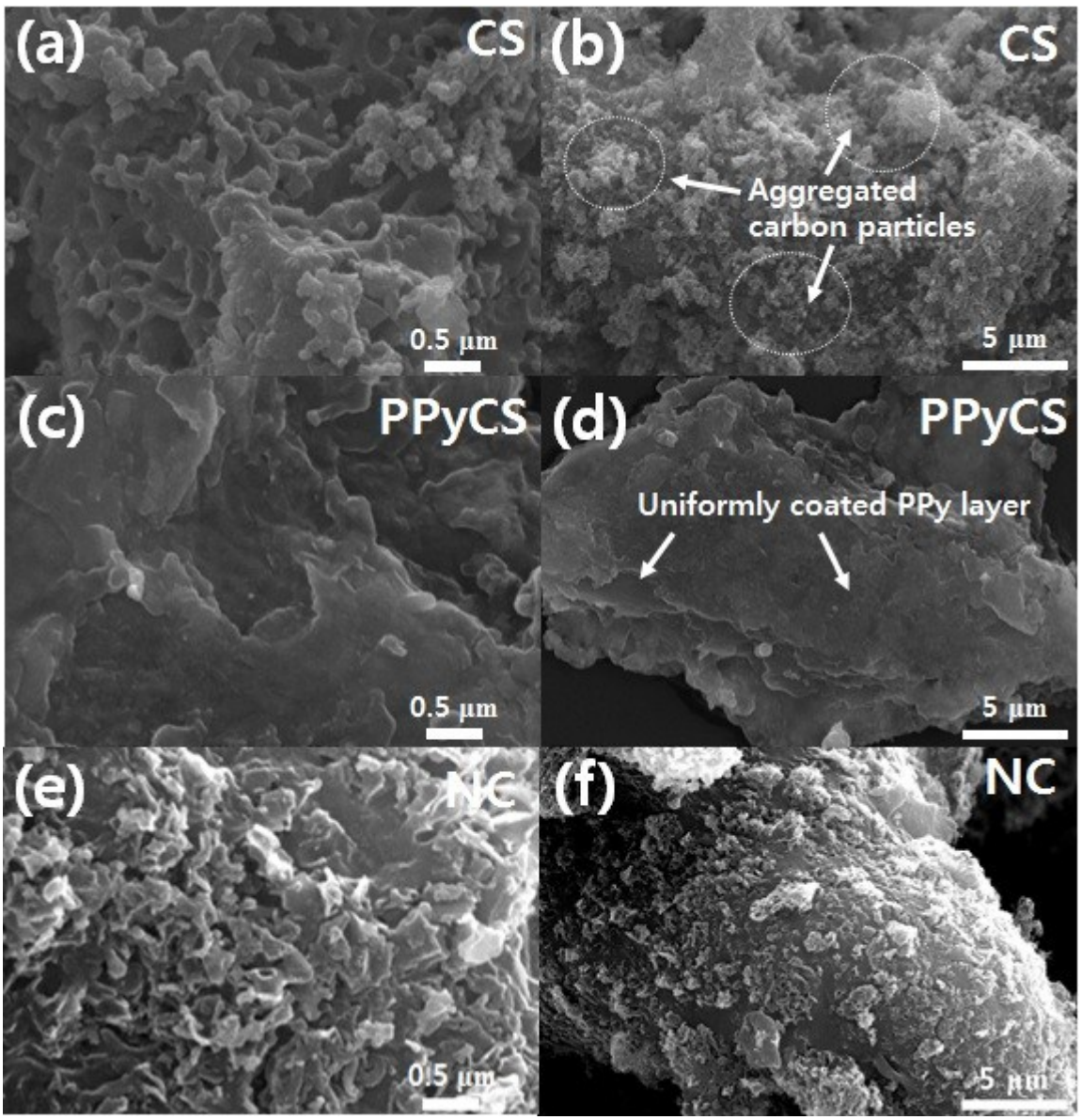

Fig. S1 SEM images of (a)-(b) CS, (c)-(d) PPyCS and (e)-(f) NC.

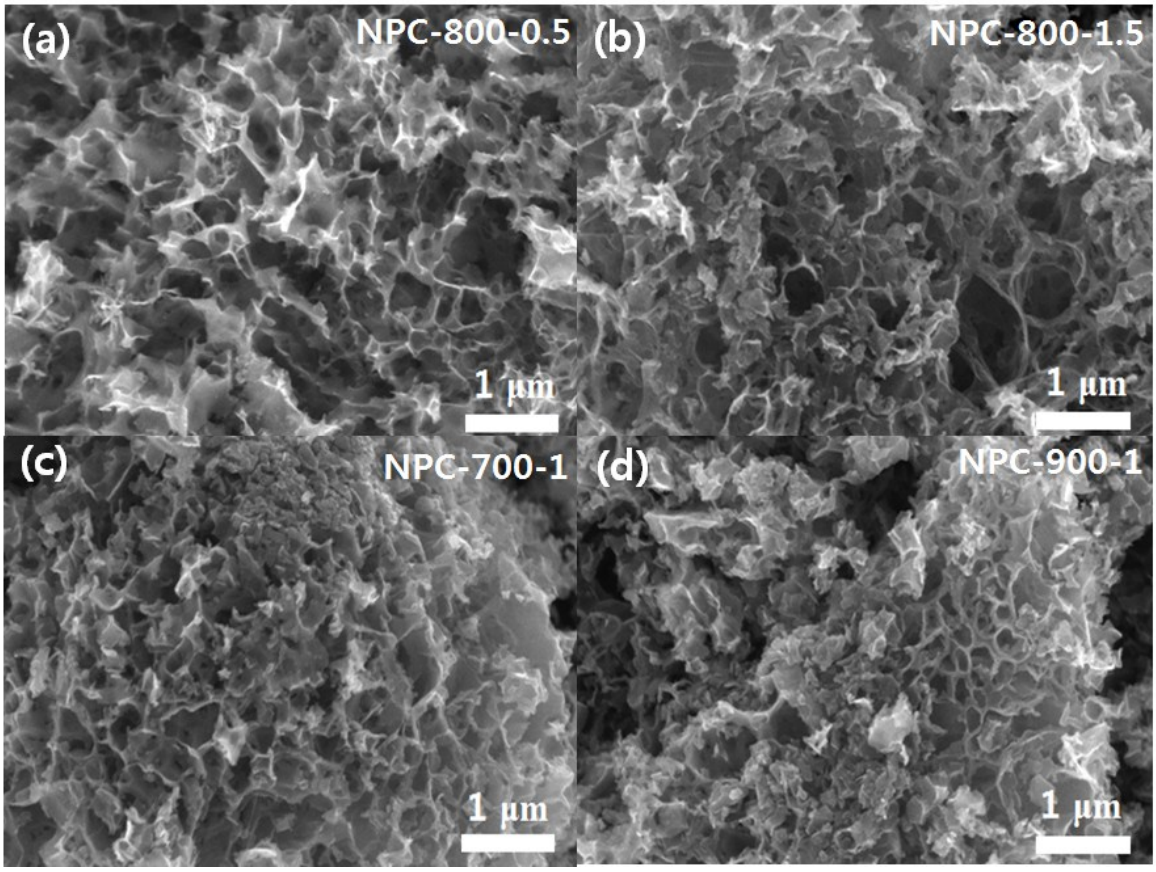

Fig. S2 SEM images of (a) NPC-800-0.5, (b) NPC-800-1.5, (c) NPC-700-1 and (d) NPC-900-1.

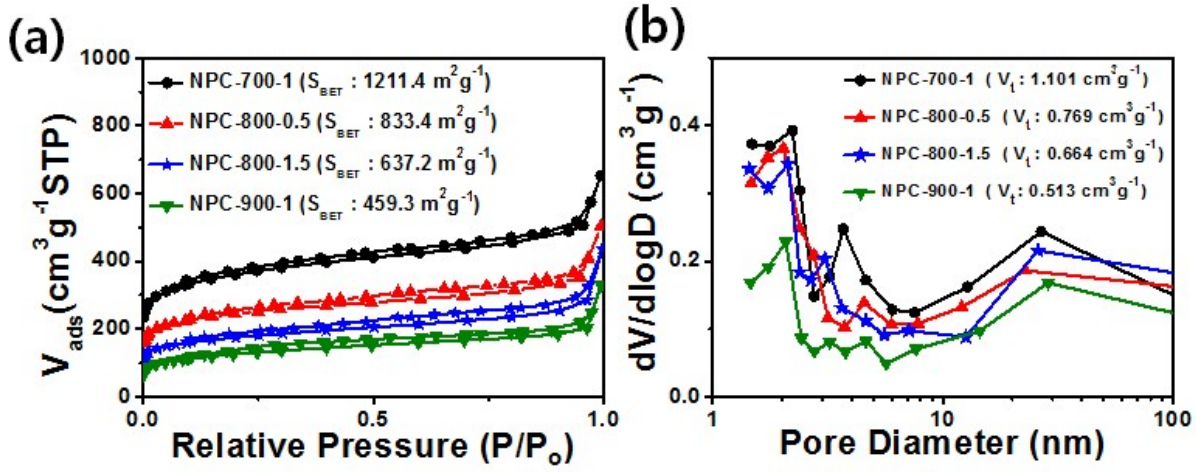

Fig. S3 (a) N_2 sorption isotherms and (b) the corresponding pore size distributions of various N-doped porous carbons.

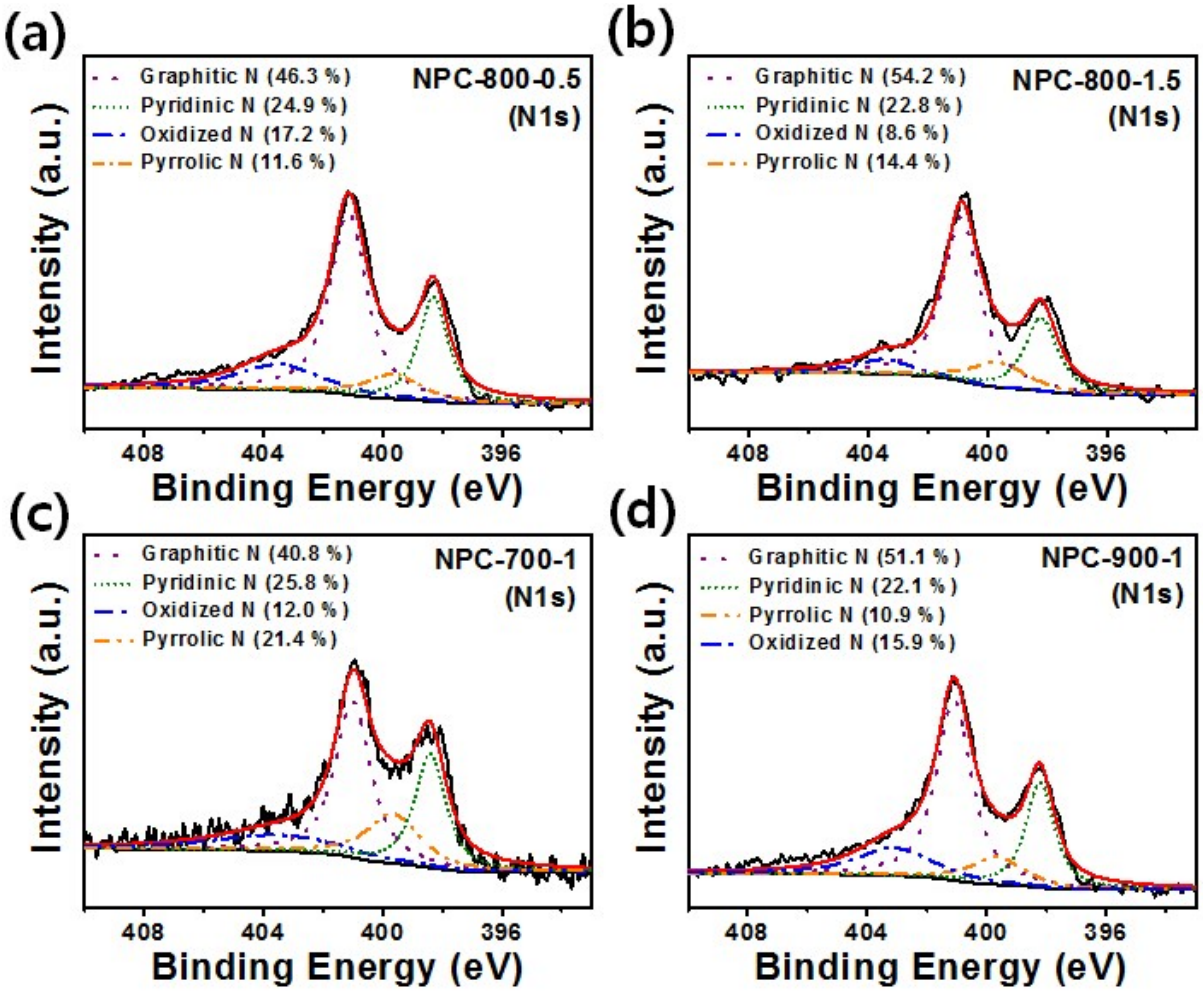

Fig. S4 XPS survey spectra and high resolution N 1s spectra of (a) NPC-800-0.5, (b) NPC-800-1.5, (c) NPC-700-1 and (d) NPC-900-1.

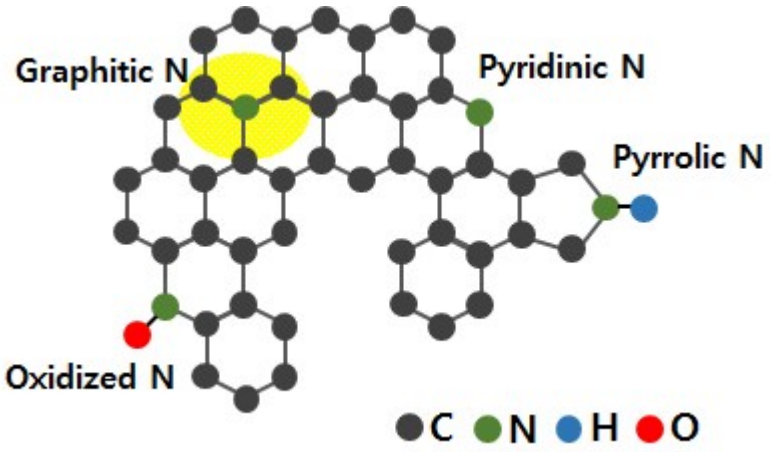

Fig. S5 Schematic illustration of different bonding configurations in the N doped carbon structure.

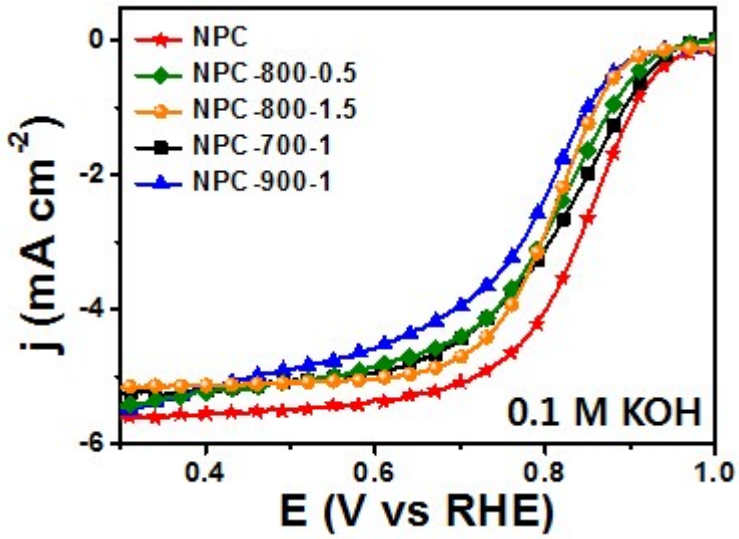

Fig. S6 ORR polarization curves of various N-doped porous carbons prepared under different activation parameters.

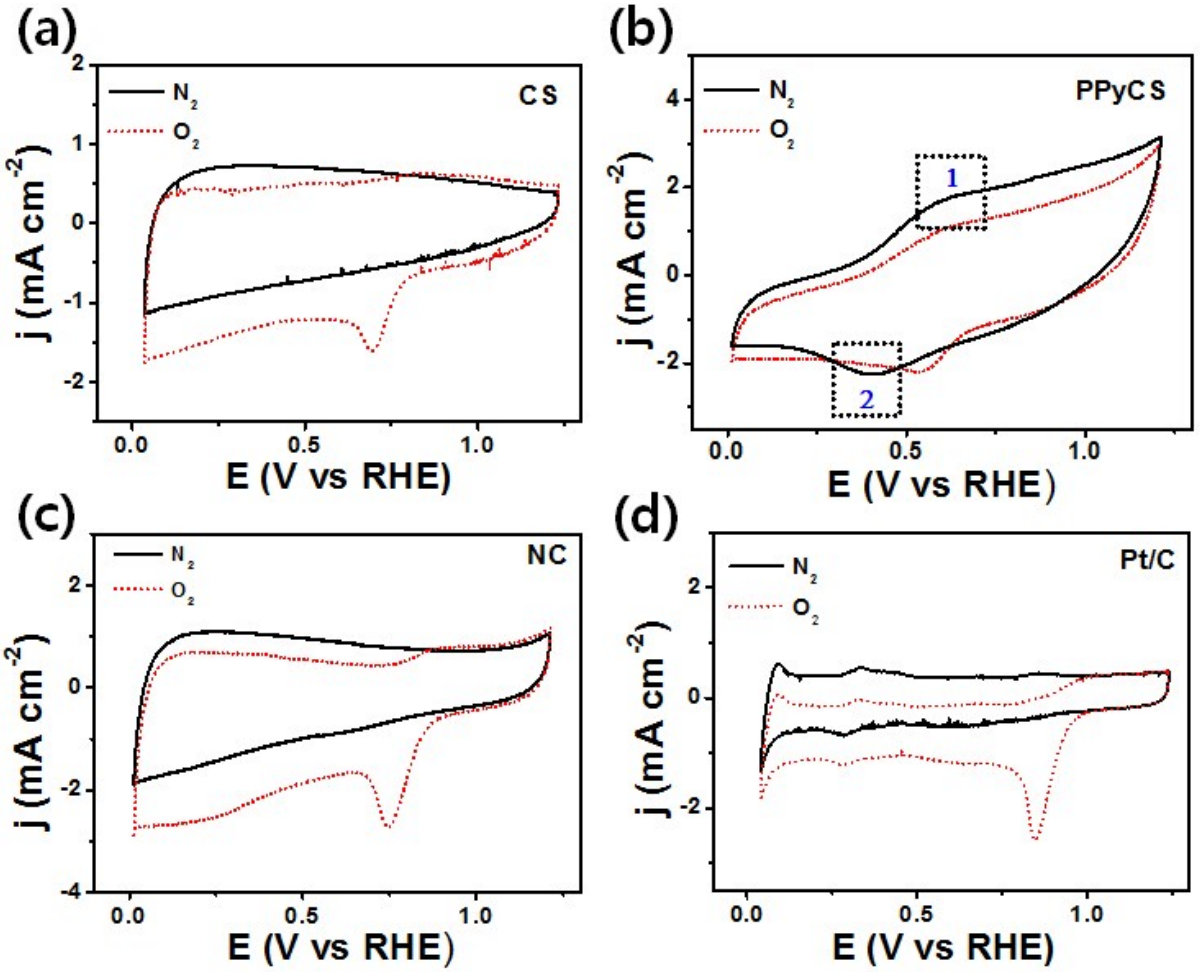

Fig. S7 CV curves of (a) CS, (b) PPyCS, (c) NC and (d) Pt/C in 0.1 M KOH electrolyte saturated with N_2 or O_2 at a scan rate of 50 mV s^{-1}.

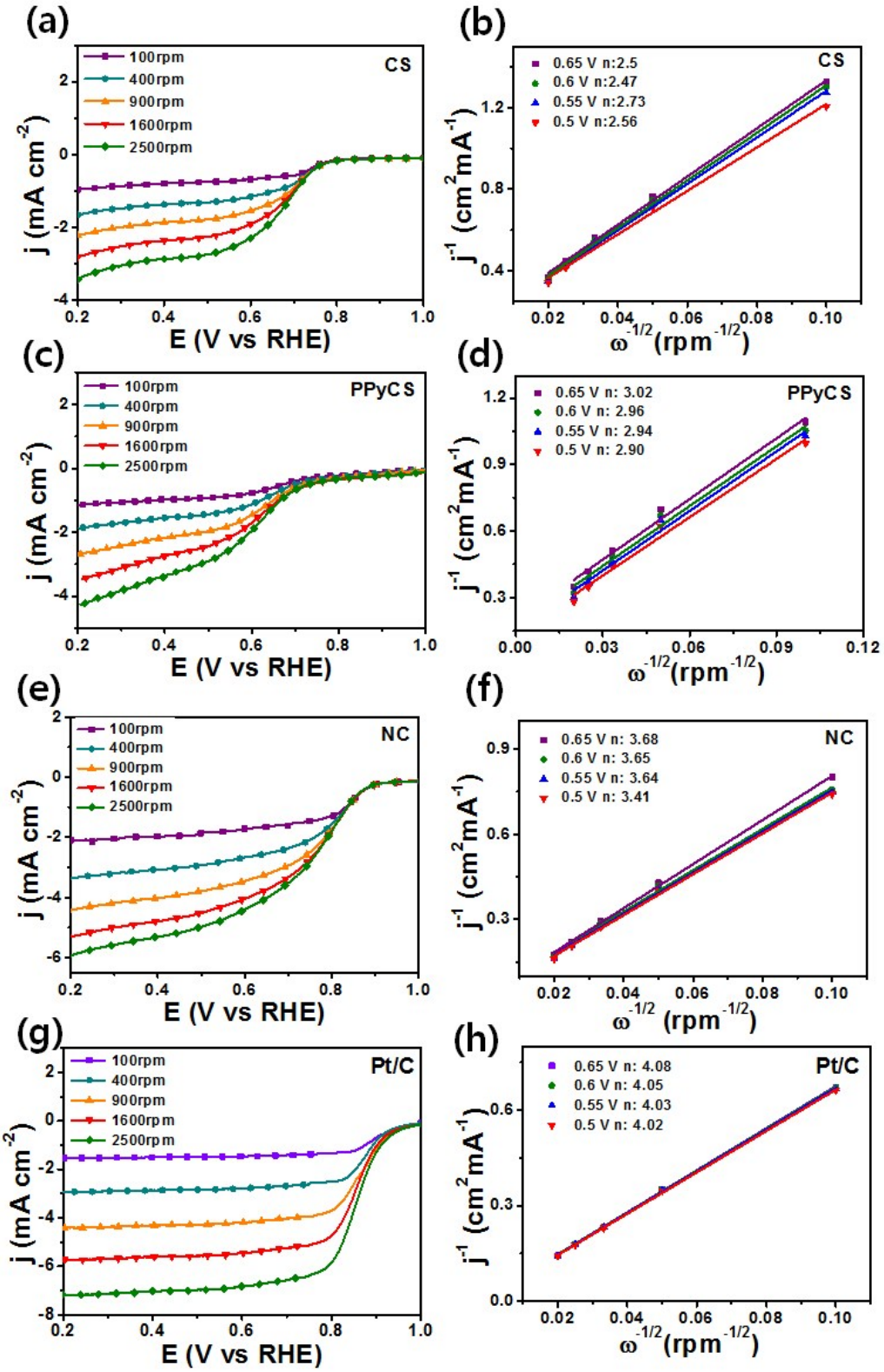

Fig. S8 ORR polarization curves of (a) CS, (c) PPyCS (e) NC and (g) Pt/C in 0.1 M KOH electrolyte under different rotating rates and the corresponding Koutecky-Levich plots of (b) CS, (d) PPyCS (f) NC and (h) Pt/C at different potentials.

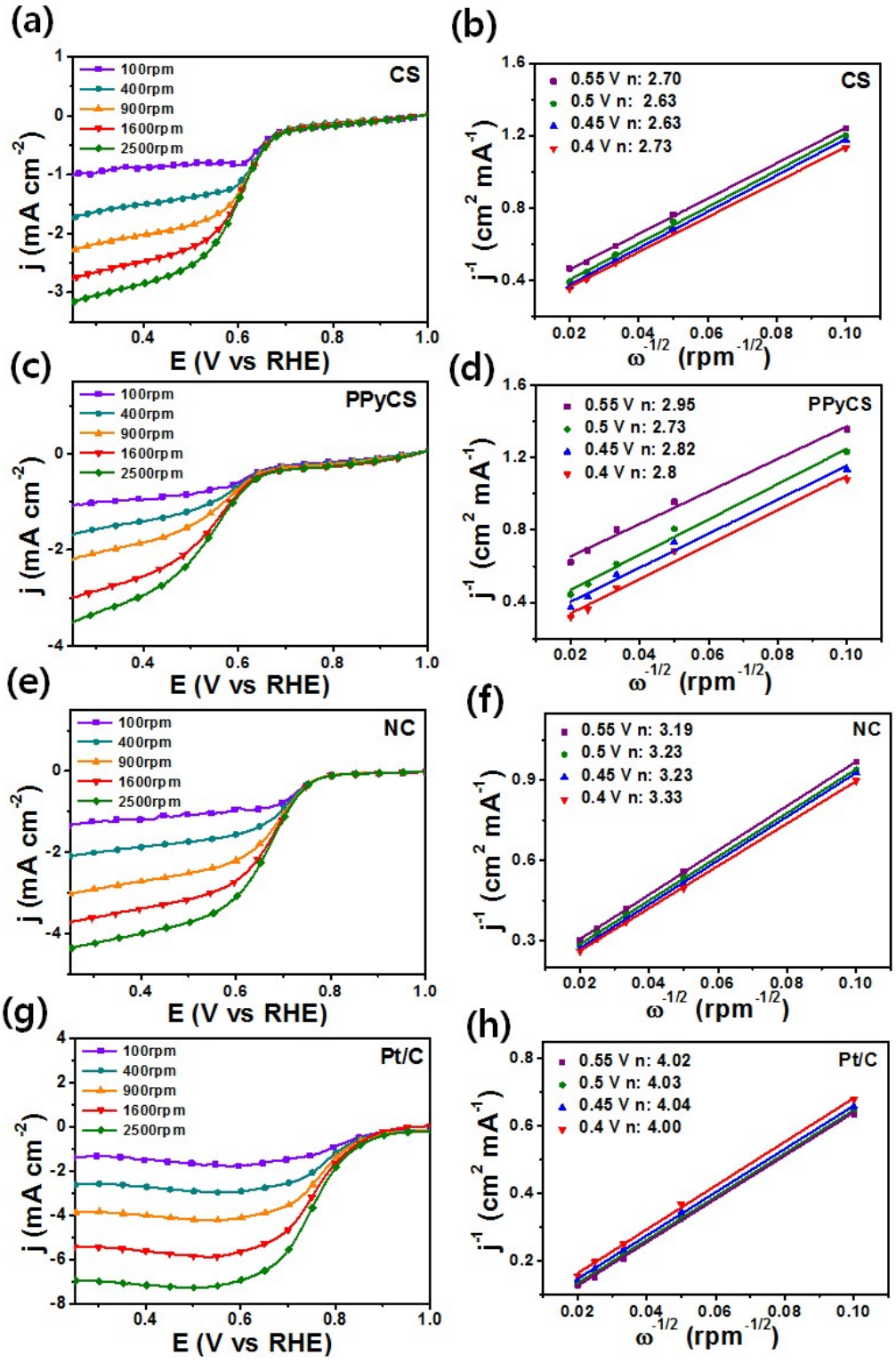

Fig. S9 ORR polarization curves of (a) CS, (c) PPyCS (e) NC and (g) Pt/C in 0.5 M H_2SO_4 electrolyte under different rotating rates and the corresponding Koutecky-Levich plots of (b) CS, (d) PPyCS (f) NC and (h) Pt/C at different potentials.

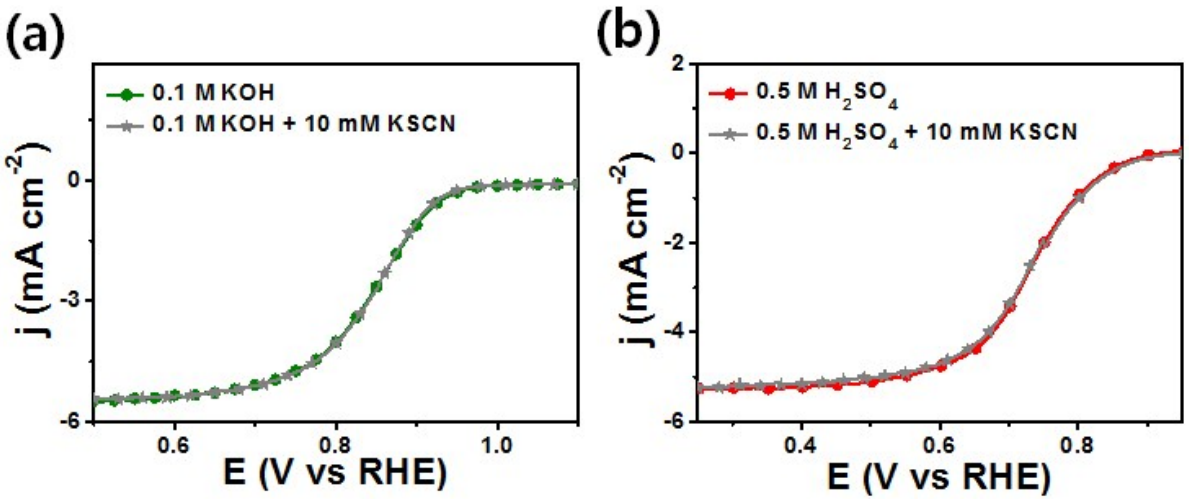

Fig. S10 ORR polarization curves of NPC in (a) 0.1 M KOH electrolyte (with and without 10 mM KSCN) and (b) 0.5 M H_2SO_4 electrolyte (with and without 10 mM KSCN) saturated with O_2 at a scan rate of 10 mV s^{-1} under 1600 rpm.

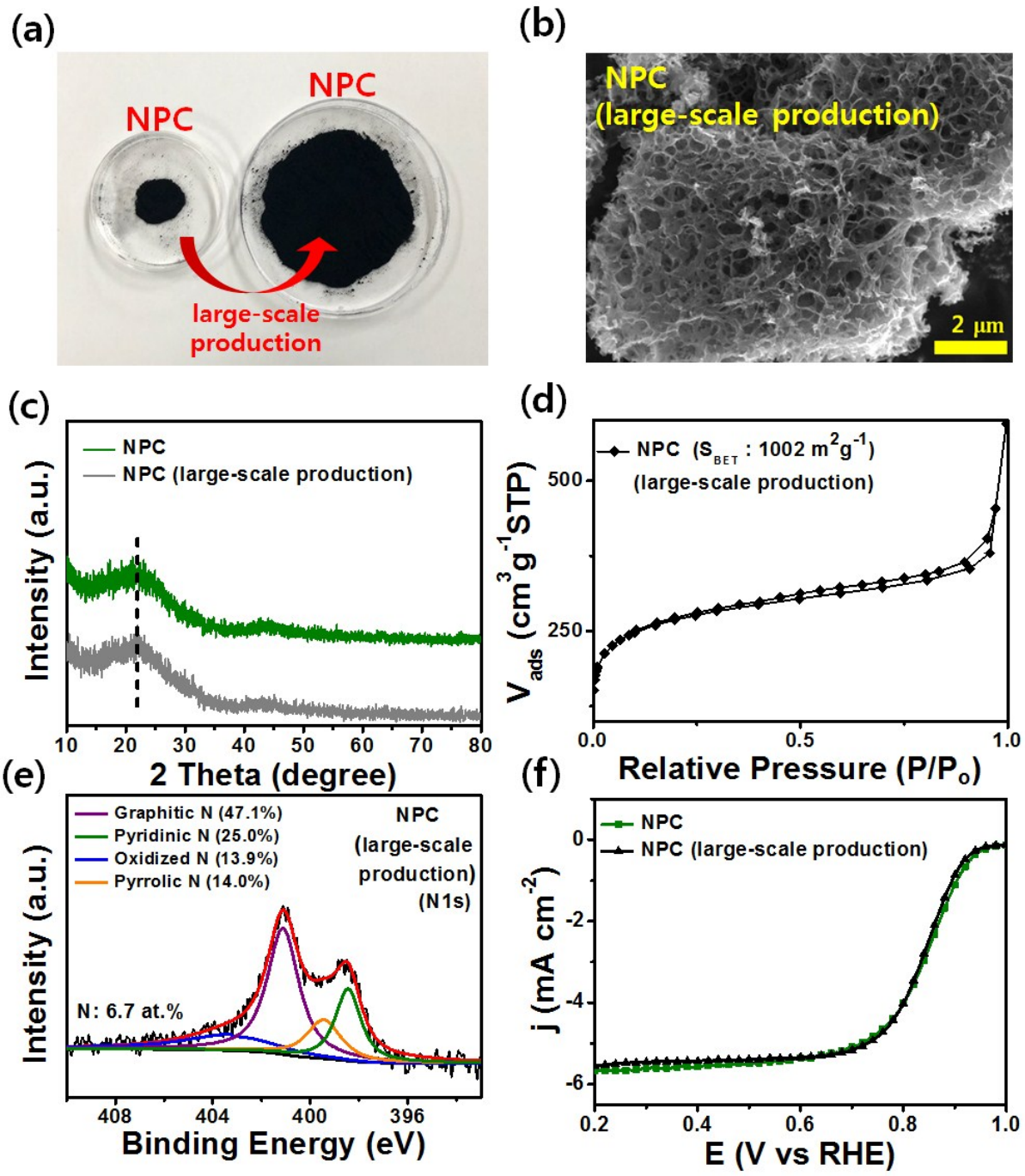

Fig. S11 (a) Photograph of NPC and NPC (large-scale production), (b) SEM image, (c) XRD patterns, (d) N_2 sorption isotherm, (e) high resolution N 1s spectra and (f) ORR activity of NPC (large-scale production).